Compressible metamagnetic Ising model: Mean-field Curie-Weiss approach and Landau expansion

A. F. S. Moreira*
Centro de Ciências Tecnológicas da Terra e do Mar, Universidade do Vale do Itajaí, Itajaí, SC, Brazil

W. Figueiredo†
Departamento de Física, Universidade Federal de Santa Catarina, 88040-900 Florianópolis, SC, Brazil

Vera B. Henriques‡
Instituto de Física, Universidade de São Paulo, Caixa Postal 66318, 05389-970 São Paulo, SP, Brazil
(Received 9 August 2002; published 31 December 2002)

A layered compressible metamagnetic Ising model is studied within the mean-field Curie-Weiss approach and the Landau expansion. The ferromagnetic and antiferromagnetic couplings depend linearly on the volume as in Domb's ferromagnetic model. For equal spin-lattice couplings of ferromagnetic and antiferromagnetic interactions a closed solution is obtained, suitable for arbitrary values of the compressibility. For a large spin-lattice coupling and a high compressibility, two tricritical points appear in the magnetic field-temperature phase diagram, one at low temperatures, and other at high temperatures, for a low hydrostatic pressure. For an arbitrary ratio of the spin-lattice couplings a perturbation expansion of the free energy on the inverse elastic constant is presented. The effect of pressure on the single tricritical point comprises three possibilities, according to the signs of the derivatives of the tricritical temperature and field, related to the magnitude of the ferromagnetic/antiferromagnetoelastic couplings. In the experimental literature there are some compressible metamagnets whose tricritical behaviors as a function of pressure are in agreement with these findings.

DOI: 10.1103/PhysRevB.66.224425 PACS number(s): 75.80.+q, 64.60.Cn, 64.60.Kw

I. INTRODUCTION

The phase diagram of metamagnetic systems in the magnetic field versus temperature plane has been studied both theoretically[1–8] and experimentally.[9–12] The phase diagram exhibits paramagnetic-antiferromagnetic transitions, of first order at high magnetic field, and critical at low field. These two lines often join at a tricritical point, but a more complex behavior is also possible, with coexistence between different magnetic phases.

The compressibility of ferromagnetic Ising systems was addressed in a series of theoretical studies[13–20] some time ago. For an exchange interaction linearly dependent on interion distance, an integration of elastic variables leads to an effective long-range four-spin interaction. The sign of this effective interaction is crucial for the characterization of the magnetic transition, which may be either critical, with pure or renormalized Ising exponents,[14,19] or discontinuous in both magnetic and number densities.[15–18] Two simple limiting cases correspond to zero[14] and infinite[13] shear forces: in the first case both the elastic and magnetic couplings depend only on the longitudinal component of the relative positions of the ions, and in the second position fluctuations are absent and interion distances are volume dependent. The Baker-Essam model presents Ising critical indices under constant pressure and Ising renormalized critical indices at constant volume.[14,19] As for Domb's model, a mean-field approach and $2d$ exact or renormalization-group treatments produce qualitatively different results: a tricritical point in the temperature-pressure plane is present in the first case, and only first-order transitions in the second case. Interestingly, the inclusion of finite shear through fluctuation of bond lengths does not stabilize the critical behavior in cases of the isotropic[17] and cubic elastic lattices;[16] therefore a Domb-like behavior prevails, i.e., the magnetic transition is turned discontinuous through the elasticity of the underlying lattice. More recently, simulation studies have been carried out for an anisotropic elastic potential.[21]

A metamagnetic Ising system under pressure was considered previously,[22] in the spirit of the shearless Baker-Essam model.[14] The phase diagram is essentially the same as that of the rigid model. The tricritical temperature was explicitly determined as a function of pressure, and possible relations to experimental results[23] were discussed. In view of the discrepancy between the behavior of the two extreme models in the case of ferromagnetism, it is of interest to consider the effect of shear stress on metamagnets.

Experimental investigations on the metamagnetic compounds $FeBr_2$ and $FeCl_2$ (Ref. 23) and $Ni(NO_3)_2.2H_2O$,[24,25] under hydrostatic pressure, have been performed. From measurements of the magnetization on these systems the dependence of the tricritical point, Néel temperature and transition field at zero temperature on pressure was determined. The model we have developed in this work aims to understand the different behaviors exhibited by these metamagnets in the experiments.

In the present study, layered metamagnets with infinite shear forces, are discussed as a function of the external pressure. We perform a Landau expansion for the model free energy in order to investigate the general effects of the compressibility on the critical behavior. We also compare our results with some experimental data found in the literature. This paper is organized as follows: in Sec. II we present the model Hamiltonian. In Sec. III we perform a mean-field transformation. In Sec. IV we derive the Landau expansion. Section V is devoted to a discussion of the isotropic spin-lattice couplings, and in Sec. VI we address the corresponding anisotropic case and compare our results with the experimental data. Finally, in Sec. VII, we present our conclusions.

II. MODEL HAMILTONIAN

The compressible metamagnetic model we consider exhibits the same elastic features of Domb's ferromagnetic model.[13] The deformations are homogeneous and isotropic (infinite shear forces). The magnetic interactions are considered through an Ising spin system on a cubic lattice, in d space dimensions, constituted by two sublattices. The sublattices are chosen to be the alternating layers of $d-1$ dimensions of the lattice. The exchange interaction between first neighboring spins on the same sublattice is of the ferromagnetic type, while the coupling between neighboring spins belonging to different sublattices is of the antiferromagnetic type. Our choice of stacking planes for the sublattices is motivated by the crystalline structure of some metamagnetic compounds like $FeBr_2$ and $FeCl_2$. They are composed of hexagonal sheets of Fe^{2+} spins, which at low temperature are ferromagnetically aligned along the hexagonal c axis, whereas successive sheets are stacked antiferromagnetically. However, we could started with another representation for the sublattices, but the results within the mean-field approach would be essentially the same. The Hamiltonian of the model is given by

$$\mathcal{H}=-\frac{1}{2}\sum_{ij}\sigma_i[J_{ij}-j_{ij}(a-a_0)]\sigma_j+\frac{1}{2}\sum_{ij}\frac{1}{2}K(a-a_0)^2-\sum_i H_i\sigma_i, \tag{1}$$

where $\sigma_i=\pm 1$ are the spin variables, and a_0 is the average distance between neighboring spins at a reference temperature T_0. H_i is the magnetic field on site i. The second term on the right is the elastic energy of the lattice, represented by the harmonic potential between nearest-neighbor pairs of spins, where K is the elastic constant and a is the average distance between neighboring spins at temperature T. We assume a linear approximation for the dependence of the exchange couplings on the lattice constant a, justified for very large values for K, so that only small lattice deformations are considered.

The partition function at constant volume $\mathcal{Z}_a(T,a,N,H_i)$, can be transformed in order to introduce the pressure into the problem. This is done by making a Laplace transformation to the pressure ensemble,

$$\mathcal{Z}=\int_{-\infty}^{+\infty}dV\exp(-\beta pV)\mathcal{Z}_a(T,a,N,H_i), \tag{2}$$

where $\beta=1/(k_BT)$, V is the volume of the system and p its pressure. Let us expand the volume around the reference volume at T_0, $V=Na_0^d[1+d/a_0(a-a_0)+O((a-a_0)^2)]$, keeping only first-order contribution. Integrating over $(a-a_0)$ we obtain

$$\mathcal{Z}(T,p,N,H_i)=c\exp[-\beta N\mathcal{H}_0(p)]\mathcal{Z}_\sigma, \tag{3}$$

where

$$c=dNa_0^{d-1}\sqrt{\frac{2\pi}{dN\beta K}},\quad \mathcal{H}_0(p)=pa_0^d-\frac{1}{2}d\frac{a_0^{2(d-1)}p^2}{K}, \tag{4}$$

$$\mathcal{Z}_\sigma=\sum_{\{\sigma\}}\exp(-\beta\mathcal{H}'), \tag{5}$$

and

$$\mathcal{H}'=-\frac{1}{2}\sum_{ij}\sigma_i\left(J_{ij}+\frac{pa_0^{d-1}}{K}j_{ij}\right)\sigma_j-\frac{1}{2}\left(\sum_{ij}\sigma_i\frac{j_{ij}}{2\sqrt{dNK}}\sigma_j\right)^2-\sum_i H_i\sigma_i. \tag{6}$$

We note that the transformation to the pressure ensemble introduces a biquadratic term, which couples different pairs of spins all over the lattice.

To render the argument of the exponential more manageable in Eq. (5), we apply a Gaussian transformation to the biquadratic term,

$$\mathcal{Z}_\sigma=\sum_{\{\sigma\}}\int_{-\infty}^{+\infty}dy\times\exp\left(-\frac{y^2}{2}+\frac{1}{2}\beta\sum_{ij}\sigma_iL_{ij}\sigma_j+\beta\sum_i H_i\sigma_i\right), \tag{7}$$

where the coupling matrix is defined by

$$L_{i,j}(F,A)=\pm J_{F,A}\pm\left(\frac{pa_0^{d-1}}{K}+y\sqrt{\frac{1}{dN\beta K}}\right)j_{F,A}. \tag{8}$$

Note that our choice of signs implies an increment of the exchange interaction under compression, for positive magnetoelastic couplings $j_{A,F}$, in both the ferromagnetic and antiferromagnetic cases.

III. MEAN-FIELD FREE-ENERGY

In order to advance, we shall transform the effective spin Hamiltonian, allowing each spin to interact with all other spins in the lattice with the same strength. This is the Curie-Weiss mean-field approximation, and the notion of dimension is completely lost in the transformed system. The original lattice can be thought as a stack of ferromagnetic hyperplanes A and B, with an antiferromagnetic coupling between them. For the Curie-Weiss version of the model, where each spin of the lattice is coupled to any other, having $N/2$ ferromagnetic couplings L_F and $N/2$ antiferromagnetic ones L_A. To keep the free energy finite, the effective couplings must be taken as L_F/N and L_A/N. Notice that, unlike the real system, there is no difference in the number of ferromagnetic and antiferromagnetic couplings in this mean-field approach.

The applied field at each lattice site i is divided into two parts: a uniform positive H field and a staggered H_s field, which are positive on the A sublattice and negative on the

B sublattice. The effective spin partition function [Eq. (7)], becomes

$$\mathcal{Z}_\sigma=\sum_{\{\sigma\}}\int_{-\infty}^{+\infty}dy\,\exp-\Biggl\{\frac{y^2}{2}-\beta\frac{L_F-L_A}{4N}\Biggl(\sum_{i\in A}\sigma_i+\sum_{j\in B}\sigma_j\Biggr)^2 -\beta\frac{L_F+L_A}{4N}\Biggl(\sum_{i\in A}\sigma_i-\sum_{j\in B}\sigma_j\Biggr)^2 -\beta(H+H_s)\sum_{i\in A}\sigma_i-\beta(H-H_s)\sum_{j\in B}\sigma_j\Biggr\}. \tag{9}$$

Before we proceed with the sum over the spins variables, we consider once more the Gaussian transformation, applied to the two quadratic spin sums in the last equation. Introducing two variables x and w, we can write

$$\mathcal{Z}=\int_{-\infty}^{+\infty}dy\int_{-\infty}^{+\infty}dx\int_{-\infty}^{+\infty}dw\,\exp[-\Phi(y,x,w,T,p,H,H_s)], \tag{10}$$

where

$$\Phi=\frac{y^2}{2}+\frac{x^2}{2}+\frac{w^2}{2}-\frac{N}{2}\ln(2\cosh Q_+)-\frac{N}{2}\ln(2\cosh Q_-), \tag{11}$$

$$Q_\pm=x\sqrt{\frac{\beta(L_F-L_A)}{N}}\pm w\sqrt{\frac{\beta(L_F+L_A)}{N}}+\beta(H\pm H_s). \tag{12}$$

In the thermodynamic limit, $N\to\infty$, the main contribution to the partition function comes from the values for which the exponential function is a sharp maximum. Expanding Φ around its extreme point $(\bar{x},\bar{y},\bar{w})$ and keeping terms up to second order, we have

$$\mathcal{Z}=\int_{-\infty}^{+\infty}dy\int_{-\infty}^{+\infty}dx\int_{-\infty}^{+\infty}dw\,\exp-\{\bar{\Phi}+\Phi_{\overline{xx}}(x-\bar{x})^2+\Phi_{\overline{yy}}(y-\bar{y})^2+\Phi_{\overline{ww}}(w-\bar{w})^2+2\Phi_{\overline{xy}}(x-\bar{x})(y-\bar{y})+2\Phi_{\overline{xw}}(x-\bar{x})(w-\bar{w})+2\Phi_{\overline{yw}}(y-\bar{y})(w-\bar{w})\}, \tag{13}$$

with $\Phi_{\overline{\alpha\beta}}\equiv[\partial^2\Phi/\partial\alpha\partial\beta]_{\bar{\alpha},\bar{\beta}}$. After some algebraic manipulations, we obtain

$$\mathcal{Z}=\exp\left(-\bar{\Phi}-\frac{1}{2}\ln D\right), \tag{14}$$

$$D=\pi^{3/2}\left[\Phi_{\overline{ww}}\left(\Phi_{\overline{yy}}-\frac{\Phi_{\overline{xy}}^2}{\Phi_{\overline{ww}}}\right)\left(\Phi_{\overline{xx}}-\frac{\Phi_{\overline{xw}}^2}{\Phi_{\overline{ww}}}\right)-\Phi_{\overline{ww}}\left(\Phi_{\overline{xy}}-\frac{\Phi_{\overline{xw}}\Phi_{\overline{yw}}}{\Phi_{\overline{ww}}}\right)^2\right]. \tag{15}$$

Provided $D>0$, in the thermodynamic limit, $N\to\infty$, the contribution of the logarithmic term may be neglected, so we finally arrive at the normalized Gibbs free energy

$$g(T,p,H,H_s)=-\frac{1}{N\beta}\ln\mathcal{Z}=\frac{\bar{\Phi}}{N\beta}+\mathcal{H}_0(p), \tag{16}$$

where $\mathcal{H}_0(p)$ is defined in Eq. (4).

Let us introduce the sublattice magnetizations m_A and m_B. Then we define the total magnetization $m=(m_A+m_B)/2$ and the staggered magnetization $m_s=(m_A-m_B)/2$. The staggered magnetization m_s is the order parameter conjugate to the staggered field H_s. We can write

$$m=\frac{\partial g}{\partial H}=\frac{1}{2}\tanh(Q_+)+\frac{1}{2}\tanh(Q_-),$$

$$m_s=\frac{\partial g}{\partial H_s}=\frac{1}{2}\tanh(Q_+)-\frac{1}{2}\tanh(Q_-), \tag{17}$$

where Q_+ and Q_- are defined by Eq. (12) (for $x=\bar{x}$ and $w=\bar{w}$). Finally, from Eqs. (11) and (12), $\bar{x},\bar{y}$ and $\bar{w}$ can be written as functions of m and m_s,

$$\bar{x}=\sqrt{N\beta\left[J_-(p)+\frac{j_-}{2}(j_-m^2+j_+m_s^2)\right]}\,m,$$

$$\bar{y}=\frac{\sqrt{N\beta}}{2}(j_-m^2+j_+m_s^2),$$

$$\bar{w}=\sqrt{N\beta\left[J_+(p)+\frac{j_+}{2}(j_-m^2+j_+m_s^2)\right]}\,m_s, \tag{18}$$

where we defined

$$j_\pm=\frac{1}{\sqrt{dK}}\frac{j_F\pm j_A}{2},\qquad J_\pm=\frac{J_F\pm J_A}{2},$$

$$J_\pm(p)=J_\pm+\frac{a_0^{d-1}p}{K}\frac{j_F\pm j_A}{2}. \tag{19}$$

Now, substituting Eqs. (12) and (18) into Eq. (17), we obtain the mean-field recurrence relations for $m(T,p,H,H_s)$ and $m_s(T,p,H,H_s)$,:

$$H=-\left[J_-(p)+\frac{j_-}{2}(j_-m^2+j_+m_s^2)\right]m+\frac{1}{4\beta}\ln\left[\frac{(1+m+m_s)(1+m-m_s)}{(1-m+m_s)(1-m-m_s)}\right], \tag{20}$$

$$H_s=-\left[J_+(p)+\frac{j_+}{2}(j_-m^2+j_+m_s^2)\right]m_s+\frac{1}{4\beta}\ln\left[\frac{(1+m+m_s)(1-m+m_s)}{(1+m-m_s)(1-m-m_s)}\right]. \tag{21}$$

The physical solutions of this set of coupled equations minimize the free energy and define the state of the system for fixed values of T, H and p. From Eqs. (11) and (16) we have, for the Gibbs free energy,

$$g(T,p,H,H_s)=\mathcal{H}_0(p)+\frac{1}{2}J_-(p)m^2+\frac{1}{2}J_+(p)m_s^2 + \frac{3}{8}(j_-m^2+j_+m_s^2)^2+\frac{1}{4\beta}\ln[(1+m+m_s) \times(1+m-m_s)(1-m+m_s)(1-m-m_s)]. \tag{22}$$

IV. LANDAU EXPANSION

The Landau expansion consists in developing the free energy in a power series of the order parameter, with coefficients depending only on field variables, for standard analysis.[26] So, we perform a Legendre transform on $g(T,p,H,H_s)$ [Eq. (22)] in order to replace the field H_s by the magnetization m_s. That is,

$$\Psi(T,p,H,m_s)=g(T,p,H,H_s)+H_s m_s, \tag{23}$$

where $m=m(T,p,H,m_s)$. The expansion takes the form

$$\Psi(T,p,H,m_s)=\Psi_0+\Psi_2 m_s^2+\Psi_4 m_s^4+\Psi_6 m_s^6+O(m_s^8). \tag{24}$$

The expansion of $\Psi(T,p,H,m_s)$, allows the analytical description of the phase transition between a paramagnetic phase ($m_s=0$) and an antiferromagnetic phase ($m_s\neq 0$). The expansion can also be used to describe a phase transition between two antiferromagnetic phases when the order parameter of both phases are close to zero.[27] However, in this paper, we are interested only in the transition between the paramagnetic and antiferromagnetic phases.

The critical properties of the model may be derived from the behavior of the coefficients of the expansion as a function of temperature, magnetic field and external pressure. In order to obtain explicit expressions for the coefficients Ψ_j, we first note that they are proportional to the coefficients of H_s:

$$H_s(T,p,H,m_s)=\frac{\partial \Psi}{\partial m_s}=2\Psi_2 m_s+4\Psi_4 m_s^3+6\Psi_6 m_s^5+\cdots. \tag{25}$$

We therefore expand Eq. (21) in powers of m_s. However, it is necessary also to consider $m=m(T,p,H,m_s)$, but inspection of Eq. (20) shows that it is not possible to obtain an explicit expression for m. We thus consider the expansion $m(T,p,H,m_s)=\Sigma_i \alpha_i m_s^{2i}$, where $\alpha_i=\alpha_i(T,p,H)$ and $i=0,1,2,\ldots$. Substituting this expansion for m into Eq. (20), we arrive at an expression of the form

$$H=\varphi_0+\varphi_1 m_s^2+\varphi_2 m_s^4+\varphi_3 m_s^6+O(m_s^8), \tag{26}$$

where $\varphi_i=\varphi_i(T,p,H)$. Now, after some straightforward work, the coefficients of Ψ_i can be found, as shown in Appendix A.

V. ISOTROPIC SPIN-LATTICE COUPLING

Let us first consider the particular situation in which the ferromagnetic and antiferromagnetic exchange interactions have the same volume dependence, that is, $j_F=j_A$. In this case $j_-=0$, and the continuous phase boundary between the antiferromagnetic and paramagnetic phases is easily obtained after the field variables are rescaled by the pressure. We define

$$t_p=\frac{k_B T}{J_+(p)},\quad h_p=\frac{H}{J_+(p)},\quad \epsilon_p=\frac{J_F+a_0^{d-1}pj_F/K}{J_A+a_0^{d-1}pj_A/K}, \tag{27}$$

where t_p and h_p are the rescaled temperature and field, and ϵ_p is the competition parameter between ferromagnetic and antiferromagnetic interactions for each value of the pressure.

From the Landau theory of phase transitions, the continuous transition is obtained for $\Psi_2=0$, which defines a relationship among t_p, h_p and ϵ_p. Equation (A5) gives $[\alpha_0]_c=\sqrt{1-[t_p]_c}$. Substituting this result in Eq. (A2), for the phase boundary we find

$$[h_p]_c=-\frac{\epsilon_p-1}{\epsilon_p+1}[\alpha_0]_c+\frac{[t_p]_c}{2}\ln\frac{1+[\alpha_0]_c}{1-[\alpha_0]_c}, \tag{28}$$

where the c index refers to the criticality. The Néel temperature t_N is given by $[h_p]_c=[\alpha_0]_c=0$, which in our case reduces to $t_N(p)=[t_p]_c=1$.

An analysis of the sign of the fourth order coefficient Ψ_4 allows one to establish the limits of stability of the phase boundary [Eq. (28)]. On the critical surface,

$$\frac{\Psi_4}{J_+(p)}=\frac{1}{4[t_p]_c^2}\left(\epsilon_p t-\epsilon_p+\frac{1}{3}\right)-\frac{\xi_p}{4}, \tag{29}$$

where $\xi_p=j_+^2/2J_+(p)$. The phase boundary is stable only for $\Psi_4>0$. The line of critical points ends at a tricritical point at $\Psi_4=0$. This point is stable only if the next coefficient of the expansion, Ψ_6, is positive, which is true for all values of pressure such that $\epsilon_p>0.6$. On the other hand, for $\epsilon_p<0.6$ the line of critical points ends at a critical endpoint.

In this work we will focus our attention only on tricritical behavior. For $\epsilon_p>0.6$ and $\Psi_2=\Psi_4=0$ we find

$$[t_p]_t^{\pm}=\frac{1}{2\xi_p}\left[\epsilon_p\pm\sqrt{\epsilon_p^2-4\xi_p\left(\epsilon_p-\frac{1}{3}\right)}\right], \tag{30}$$

where $[t_p]_t^{\pm}$ are the temperatures of two possible tricritical points as functions of pressure, subject to the condition $[t_p]_t^{\pm}\leqslant 1$,.

The different possibilities for the system's phase diagrams are summarized in the ξ_p versus ϵ_p plane, as shown in Fig. 1. Three regions are seen, divided by the dashed ($\xi_p=\frac{1}{3}$) and solid ($\xi_p^0=\epsilon_p^2/[4(\epsilon_p-\frac{1}{3})]$) lines. The corresponding typical phase diagrams are sketched in the insets. In region F, either $\Psi_4<0$ or $[t_p]_t^{\pm}\geqslant 1$, and the system exhibits only phase coexistence. For $\xi_p<\frac{1}{3}$ (area A), $[t_p]_t^{+}>1$ and the system exhibits a phase diagram typical of the rigid metamagnetic system,[10] with a single tricritical point, whose temperature

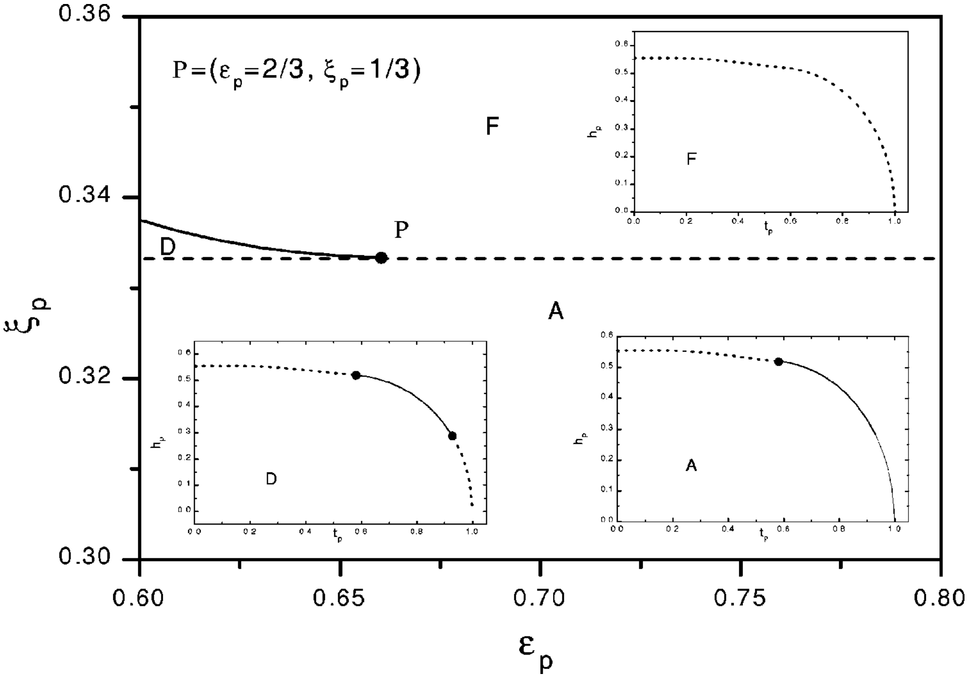

FIG. 1. Diagram in the plane ξ_p vs ϵ_p and sketch of the possible tricritical points. The insets represent typical phase diagrams corresponding to *A*, *D*, and *F* regions.

increases with ξ_p. For $\epsilon_p > \frac{2}{3}$, $[t_p]_t^- \to 1$ when $\xi_p \to \frac{1}{3}$ and the critical line disappears. For $\epsilon_p < \frac{2}{3}$ and $\frac{1}{3} < \xi_p < \xi_p^0$ (region D), both roots are physically valid and so a second tricritical point which interrupts the critical line is present. The phase diagram presents a continuous transition line between $[t_p]_t^-$ and $[t_p]_t^+$, but of course, no Néel temperature. Approaching the superior limit of region D—the solid line—we have $\lim_{\xi_p \to \xi_p^0}[t_p]_t^- = [t_p]_t^+$, and the two tricritical points collapse into one, onto a coexistence line.

In order to analyze the effect of pressure on the phase diagram, we use Eq. (19) to introduce variables

$$t = \frac{k_B T}{J_+}, \quad h = \frac{H}{J_+}, \quad \epsilon = \frac{J_F}{J_A},$$

$$g_\pm = \frac{j_\pm}{\sqrt{2J_+}}, \quad \Pi = \sqrt{\frac{2d}{KJ_+}} a_0^{d-1} p, \tag{31}$$

where t, h, and ϵ are the pressure independent reduced variables. Note that $g_- = 0$ in the isotropic case studied in this section. Π is the appropriate stress variable. Also, in terms of the variables, we have

$$\xi_p = \frac{g_+^2}{1 + g_+ \Pi}, \quad \epsilon_p = 1 + \frac{\epsilon - 1}{1 + (1+\epsilon) g_+ \Pi}. \tag{32}$$

We want to analyze the evolution of the critical behavior within the $\xi_p \times \epsilon_p$ parameter space (Fig. 1) in terms of the physical pressure.

For vanishing temperature, there is coexistence between the paramagnetic ($m = 1$, $m_s = 0$) and antiferromagnetic ($m = 0, m_s = 1$) phases, which must have the same free energy, $\Psi(T=0,p,H,m_s=0) = \Psi(T=0,p,H,m_s)$, at zero staggered field. From Eq. (23), we have, for the phase boundary at null temperature,

$$h_{(t=0)} = \frac{1}{\epsilon + 1} + \frac{g_+^2}{4} + \frac{g_+ \Pi_{(t=0)}}{2}. \tag{33}$$

At the $h = 0$ plane, if the transition is continuous, the Néel temperature exhibits a linear dependence on pressure given by $t_N = 1 + g_+ \Pi$. On the other hand, if a coexistence of phases is observed at zero field, we must impose equality of free-energies and solve mean-field equations (20) and (21). The magnetization $m = 0$ automatically satisfies Eq. (20), and Eq. (21) yields, for $H_s = 0$,

$$\frac{t_{(h=0)}}{2} \ln \frac{1 + m_s}{1 - m_s} - [1 + g_+ \Pi + g_+^2 m_s^2] m_s = 0. \tag{34}$$

The free energy [Eq. (23)] for $\Psi(T,p,H=0,m_s=0) = \Psi(T,p,H=0,m_s)$ leads to

$$(1 + g_+ \Pi) m_s^2 + \frac{g_+^2}{2} m_s^4 - t_{(h=0)}[(1+m_s)\ln(1+m_s) + (1-m_s)\ln(1-m_s)] = 0. \tag{35}$$

An analytic expression for the phase boundary at zero field as a function of the pressure, may be written, for small m_s, as

$$1 + g_+ \Pi = t_{(h=0)} - \frac{5}{48 t_{(h=0)}} (3g_+^2 - t_{(h=0)})^2; \tag{36}$$

otherwise Eqs. (34) and (35) may be solved numerically.

In Fig. 2, we exhibit the phase diagram of the model for some values of the reduced pressure Π, for particular values of the magnetic competition parameter ϵ and the magneto-elastic parameter $g_+^2 \sim j^2/K$ (respectively, 1 and 0.7^2). This corresponds to running vertically from the F to A region in Fig. 1, at $\epsilon_p = 1$. At low pressures the whole phase boundary corresponds to first-order transitions, and the more usual

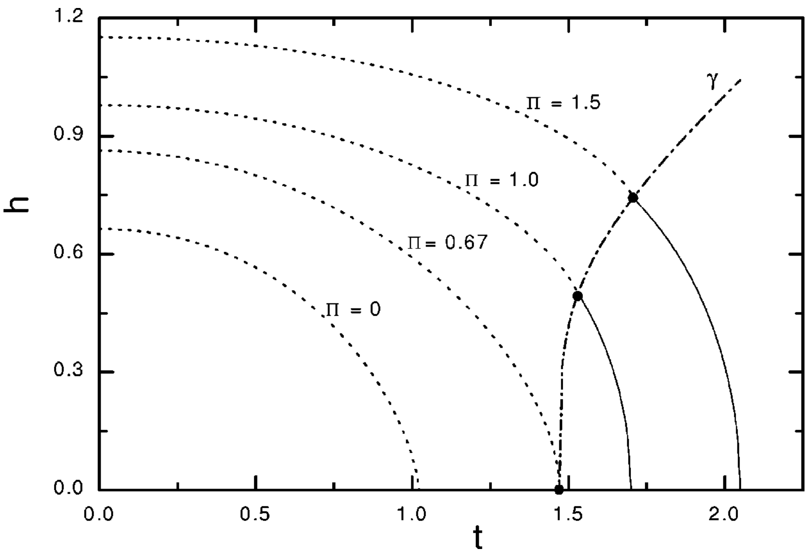

FIG. 2. Phase diagram in the plane magnetic field versus temperature for $\epsilon=1$, $g_+=0.7$ and four representative pressures. Dotted lines represent first-order transitions and full lines continuous transitions. The dashed line γ is a locus of tricritical points. The full circles are the tricritical points at the selected pressures Π. At pressure $\Pi=0.6714$ a tricritical point appears for $h=0$, a behavior analogous to that of Domb's ferromagnetic model.

metamagnetic phase diagram arises at higher pressures. A tricritical point in the temperature-pressure plane $(h=0)$ separates the two regimes. For lower values of the magnetoelastic parameter $(g_+<0.58)$, which may also be associated with low compressibility, only the usual behavior would be observed. Phase diagrams with two critical points (as in region D of Fig. 1), would be observed for large magnetoelastic couplings and small competition parameter $(\epsilon<2/3)$, at low pressures.

The behavior of the compressible metamagnetic model at zero field is reminiscent of that of Domb's ferromagnetic model under a mean-field treatment: at low pressures the compressible model exhibits first-order transitions, while continuous transitions appear at higher pressures.[19,20] There is an important difference, however, since for small spin-lattice couplings the transition is critical even for zero pressure. It remains to be seen whether fluctuations could destroy the stability of the continuous transition, as is the case for the ferromagnetic model.[17]

VI. ANISOTROPIC LOW COMPRESSIBILITY LIMIT

Let us consider the general case where $g_-\neq 0$, in the low compressibility limit (large K). The critical condition $\Psi_2=0$, with reduced variables defined by Eq. (31) in Eq. (A5) yields

$$g_-g_+\alpha_{0c}^4+(1+g_+\Pi-g_-g_+)\alpha_{0c}^2-1-g_+\Pi+t_c=0, \tag{37}$$

where the index c refers to criticality. Our definition of the effective magnetic model under pressure [Eq. (6)] relies on large values for the elastic constant K. The terms such as $g_\pm^2$ and $g_+\Pi$ are of order K^{-1}, so we solve Eq. (37) for α_{0c} and perform a perturbation expansion in those variables up to that order, obtaining

$$\alpha_{0c}=\sqrt{1-t_c(1-g_-g_+-g_+\Pi)-g_-g_+t_c^2}. \tag{38}$$

Substituting in Eq. (A2), we obtain the critical surface equation:

$$h_c=-\left(\frac{\epsilon-1}{\epsilon+1}+g_-\Pi\right)\alpha_{0c}-g_-\alpha_{0c}^3+\frac{t_c}{2}\ln\frac{1+\alpha_{0c}}{1-\alpha_{0c}}. \tag{39}$$

The Néel temperature is easily obtained. Making $h_c=0$ in Eq. (39), the unique solution is $\alpha_{0c}=0$. Equation (37) then yields the Néel temperature $t_N=1+g_+\Pi$, which has the same functional form as for the isotropic case. The dependence of the Néel temperature on the pressure is also observed in the experiments. For instance, it increases with pressure for the metamagnetic systems $FeCl_2$ (phases I and II), $FeBr_2$,[23] and $Ni(NO_3)_2.2H_2O$,[24,25] indicating that for these materials g_+ should be taken as positive.

To allow for a tricritical point on the critical line we must look at the condition $\Psi_4=0$. From Eq. (A6) we have, in terms of our variables [Eq. (31)],

$$2\left[-g_-g_++\frac{t_t}{(1-\alpha_{0t}^2)^2}\right]\alpha_{0t}\alpha_{1t}=g_+^2-\frac{t_t}{3}\frac{1+3\alpha_{0t}^2}{(1-\alpha_{0t}^2)^3}, \tag{40}$$

where the subscript t denotes the tricritical point. By taking Eqs. (A3), (38), and (40) and expanding up to order K^{-1}, we arrive at the following expression for the tricritical temperature:

$$\begin{aligned} t_t=\left(1-\frac{1}{3\epsilon}\right)\Bigg\{1&+\left[\frac{5\epsilon^2-2\epsilon+1}{2\epsilon(3\epsilon-1)}g_++\frac{(\epsilon+1)^2}{2\epsilon(3\epsilon-1)}g_-\right]\Pi\\ &+\frac{21\epsilon^3+7\epsilon^2+17\epsilon+5}{6\epsilon^2(3\epsilon-1)}g_-g_+\\ &+\frac{(\epsilon+1)^2}{2\epsilon^2(3\epsilon-1)}g_-^2+\frac{(3\epsilon-1)}{3\epsilon^2}g_+^2\Bigg\}. \end{aligned} \tag{41}$$

The line of coexistence can be found only numerically, except at $t=0$, where internal energies of the paramagnetic

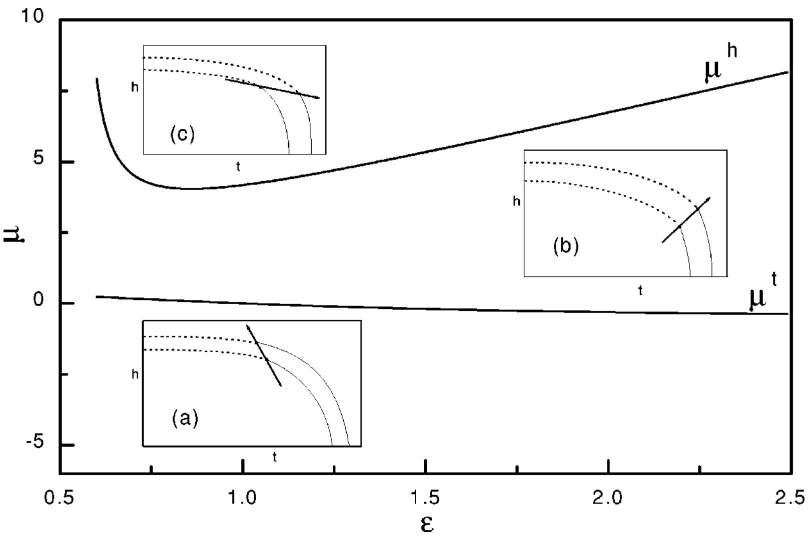

FIG. 3. Phase diagram in the plane μ (ratio of ferro and antiferro spin-lattice couplings versus ϵ. μ^t and μ^h are defined by Eqs. (B2) and (B5), respectively. The arrow in the insets indicates the direction of increasing pressures. The regions (a), (b) and (c) are associated with the behaviors of the derivatives of the tricritical temperature and field relative to the pressure.

(P) and antiferromagnetic (AF) phases become identical at the transition. From Eq. (23), the coexistence field is given by

$$h_{t=0}=\frac{1}{\epsilon+1}+\frac{g_+-g_-}{2}\Pi+\frac{g_+^2-g_-^2}{4}. \tag{42}$$

As $g_+-g_-/2=j_A/\sqrt{2dKJ_+}$, the field $h_{t=0}$ changes with pressure according to the sign of j_A. Experimental work performed on the above mentioned metamagnets[23–25] showed that $h_{t=0}$ increases with pressure, indicating also that for these compounds j_A should be taken positive.

Now let us consider the dependence of the tricritical point on pressure. First, we define a parameter $\mu=j_F/j_A$ which corresponds to the ratio of ferromagnetic and antiferromagnetoelastic couplings. We have found the values of μ for which $dt_t/d\Pi=0$ and $dh_t/d\Pi=0$, $\mu^t$and μ^h, respectively. This is shown in Appendix B.

In Fig. 3 the lines μ^t and μ^h as functions of the ratio ϵ delimit regions of physical microscopic parameters which lead to a different behavior of the system as a function of pressure. We take only $\epsilon>0.6$, which corresponds to $\Psi_6>0$, in order to keep the tricritical point stable. Assuming a positive j_A, as suggested by a comparison with experiment, three different scenarios for the evolution of the tricritical point with pressure are possible: (i) an increasing field and decreasing temperature for very small (at low ϵ) or negative (at large ϵ) ferromagnetoelastic coupling, the latter implying that the magnetic energy increases as atoms approach each other; (ii) an increasing field and temperature if the ferromagnetic and antiferromagnetoelastic couplings are of the same order (this includes the symmetric case discussed in the previous section); and finally (iii) a decreasing field and increasing temperature if the antiferromagnetoelastic coupling is large. Positive g_+, as also suggested from experiment, limits behavior (i) to $\mu>-1$.

From the experimental point of view, the three kinds of phase diagram are possible. For instance, phase diagrams for $FeCl_2$ in the low-pressure rhombohedral phase compare with Fig. 3(a) (with $dt_t/d\Pi<0$ and $dh_t/d\Pi>0$), while those of the high pressure closed packed hexagonal phase, $(FeCl_2)_{II}$, fit to Fig. 3(b) ($dt_t/d\Pi>0$ and $dh_t/d\Pi>0$). The behavior of $Ni(NO_3).2H_2O$ conforms to region (c) of Fig. 3 ($dt_t/d\Pi>0$ and $dh_t/d\Pi<0$).

Our results must also be compared to those of Uda and Figueiredo,[22] obtained for a shearless compressible metamagnet. Similarly to the ferromagnetic case, a biquadratic term [see Eq. (6)] is absent in the effective pressure-dependent magnetic Hamiltonian, if shear is absent. However, differently from the ferromagnetic case, at least in the mean-field approach, both models lead to similar results for the evolution of the phase diagrams under pressure. Scenarios (i) and (ii) were obtained for the shearless model for particular numerical parameters [$\mu,\epsilon=-0.02$, 2.9 (i); 0.97, 2.3 (ii)] which fit into the corresponding regions of Fig. 3, while scenario (iii) was not considered by the authors. Are shearless and infinite shear elasticities equivalent in the case of metamagnets? Again, calculations beyond the mean field would be needed to check on this question.

VII. CONCLUSIONS

We have studied the behavior, as a function of pressure, of an Ising layered compressible metamagnetic model. The exchange coupling between nearest-neigboring spins is taken to be linearly dependent on the volume. Under the assumption of limited compressibility, the model is studied in the Curie-Weiss mean-field approximation and the free energy is determined as a function of temperature and pressure. The critical behavior is analyzed in terms of the coefficients of the corresponding Landau expansion in the staggered magnetization.

A simple solution is obtained, in the case of isotropic magnetoelastic coupling. The magnetic field versus temperature phase diagram may present some unusual features, under the effect of compression. Depending on the values of the spin-lattice coupling, compressibility, and pressure, a second first-order transition line at high temperatures and low fields appears alongside the usual low-temperature and high-field coexistence line. In such cases, a continuous transition line smoothly joins two first-order transition lines, one at low temperature, and the other at high temperatures, and two tricritical points appear in the phase diagram. In the absence of a magnetic field, we recover the classical behavior of Domb's ferromagnet, for which the transition changes from first order to continuous, for increasing pressure, with a tricritical point in the pressure-temperature plane. In view of the destabilizing effect of fluctuations on the critical transition in the case of ferromagnets, this point requires further clarification. It is to be noted, however, that differently from the ferromagnetic case, the transition is critical for small spin-lattice coupling, even at zero pressure.

For an arbitrary ratio of ferromagnetic and antiferromagnetic spin-lattice couplings μ, a closed solution for arbitrary compressibility is unavailable, and we carried out a perturbation expansion on the inverse compressibility parameter around the rigid lattice solution. This corresponds to the situation in which a Néel temperature is present at all pressures. Three different possibilities arise for the behavior of the tricritical point under pressure, depending on the value of μ and ϵ (the ratio of ferromagnetic and antiferromagnetic exchange of the rigid model). We argue that the compressible metamagnets $(FeCl_2)_I$, $(FeCl_2)_{II}$, and $Ni(NO_3).2H_2O$ may be associated with each one of these regions. Comparison with partial results for a shearless Ising metamagnet indicates that presence of shear is not as crucial as for ferromagnets.

ACKNOWLEDGMENTS

This work was supported by the Brazilian agency CNPq.

APPENDIX A: COEFFICIENTS OF THE LANDAU EXPANSION

As T,p,H and m_s are the independent variables of the problem, from Eq. (26) we can write

$$\varphi_0 = H, \quad \varphi_1 = \varphi_2 = \varphi_3 = \ldots = 0, \tag{A1}$$

which are the desired equations for $\varphi_i(T,p,H)$ yielding the coefficients $\alpha_i(T,p,H)$:

$$\varphi_0 = H = -J_-(p)\alpha_0 - \frac{j_-^2}{2}\alpha_0^3 + \frac{1}{2\beta}\ln\frac{1+\alpha_0}{1-\alpha_0}, \tag{A2}$$

$$\varphi_1 = J_-(p)\alpha_1 + \frac{3}{2}j_-^2\alpha_0^2\alpha_1 + \frac{j_-j_+}{2}\alpha_0 - \frac{1}{2\beta}\left\{\alpha_0\left[\frac{1}{(1+\alpha_0)} + \frac{1}{(1-\alpha_0)}\right] + \frac{1}{2}\left[\frac{1}{(1+\alpha_0)^2} - \frac{1}{(1-\alpha_0)^2}\right]\right\} = 0, \tag{A3}$$

$$\varphi_2 = -J_-(p)\alpha_2 - \frac{3}{2}j_-^2(\alpha_0^2\alpha_1 + \alpha_0,\alpha_1^2) - j_-j_+\alpha_1 + \frac{1}{2\beta}\left\{-\frac{1}{4}\left[\frac{1}{(1+\alpha_0)^4} - \frac{1}{(1-\alpha_0)^4}\right] + \alpha_1\left[\frac{1}{(1+\alpha_0)^3} + \frac{1}{(1-\alpha_0)^3}\right] - \frac{\alpha_1^2}{2}\left[\frac{1}{(1+\alpha_0)^2} - \frac{1}{(1-\alpha_0)^2}\right] + \alpha_2\left[\frac{1}{(1+\alpha_0)} + \frac{1}{(1-\alpha_0)}\right]\right\} = 0. \tag{A4}$$

Finally, from Eqs. (21) and (25), we obtain the proper coefficients of the expansion of the desired thermodynamic potential [Eq. (24)]:

$$2\Psi_2 = -J_+(p) - \frac{j_-j_+}{2}\alpha_0^2 + \frac{1}{2\beta}\left[\frac{1}{(1+\alpha_0)} + \frac{1}{(1-\alpha_0)}\right], \tag{A5}$$

$$4\Psi_4 = -\frac{j_+^2}{2} - j_-j_+\alpha_0\alpha_1 + \frac{1}{2\beta}\left\{\frac{1}{3}\left[\frac{1}{(1+\alpha_0)^3} + \frac{1}{(1-\alpha_0)^3}\right] - \alpha_1\left[\frac{1}{(1+\alpha_0)^2} - \frac{1}{(1-\alpha_0)^2}\right]\right\}, \tag{A6}$$

$$6\Psi_6 = -\frac{j_-j_+}{2}(2\alpha_0\alpha_2 + \alpha_1^2) + \frac{1}{2\beta}\left\{\frac{1}{5}\left[\frac{1}{(1+\alpha_0)^5} + \frac{1}{(1-\alpha_0)^5}\right] + -\alpha_1\left[\frac{1}{(1+\alpha_0)^4} - \frac{1}{(1-\alpha_0)^4}\right] + \alpha_1^2\left[\frac{1}{(1+\alpha_0)^3} + \frac{1}{(1-\alpha_0)^3}\right] - \alpha_2\left[\frac{1}{(1+\alpha_0)^2} - \frac{1}{(1-\alpha_0)^2}\right]\right\}. \tag{A7}$$

APPENDIX B: PRESSURE DERIVATIVES AT THE TRICRITICAL POINT

First we take the derivative of Eq. (41) relative to the reduced pressure:

$$\frac{dt_t}{d\Pi} = \frac{g_+ - g_-}{6\epsilon^2}[(3\epsilon^2+1)\mu + 2\epsilon(\epsilon-1)]. \tag{B1}$$

Then we observe that

$$\left(\frac{dt_t}{d\Pi}\right)_{\mu^t} = 0 \Rightarrow \mu^t = \frac{2\epsilon(1-\epsilon)}{3\epsilon^2+1}. \tag{B2}$$

We have $\mu^t = 0$ at $\epsilon = 1$. As $g_+ - g_- = 2j_A/\sqrt{2dKJ_+}$, the ratio $(dt_t/d\Pi)/j_A > (<) 0$ if $\mu > (<) \mu^t$.

The field at the tricritical point is found by inserting Eq. (41) into Eq. (A2). Its derivative with relation to pressure is given by

$$\frac{dh_t}{d\Pi} = -g_-\alpha_{0t} + \frac{1}{2}\frac{dt_t}{d\Pi}\ln\frac{1+\alpha_{0t}}{1-\alpha_{0t}} - \left[\frac{\epsilon-1}{\epsilon+1} + g_-\Pi + 3g_-^2\alpha_{0t}^2 - \frac{t_t}{1-\alpha_{0t}^2}\right]\frac{d\alpha_{0t}}{d\Pi}. \tag{B3}$$

The larger terms of this expression are of order $K^{-1/2}$. By expanding the right side in the last equation up to order $K^{-1/2}$, we obtain

$$\frac{dh_t}{d\Pi}=\frac{g_+-g_-}{2}\left\{\left[\frac{3\epsilon^2+1}{6\epsilon^2}\ln\frac{\sqrt{3\epsilon}+1}{\sqrt{3\epsilon}-1}-\frac{\epsilon+1}{\epsilon\sqrt{3\epsilon}}\right]\mu+\frac{\epsilon-1}{3\epsilon}\ln\frac{\sqrt{3\epsilon}+1}{\sqrt{3\epsilon}-1}+\frac{2}{\sqrt{3\epsilon}}\right\}. \tag{B4}$$

This derivative becomes zero at $\mu=\mu^h$, where

$$\mu^h=2\epsilon\frac{2\sqrt{3\epsilon}+(\epsilon-1)\ln\frac{\sqrt{3\epsilon}+1}{\sqrt{3\epsilon}-1}}{2(\epsilon+1)\sqrt{3\epsilon}-(3\epsilon^2+1)\ln\frac{\sqrt{3\epsilon}+1}{\sqrt{3\epsilon}-1}}. \tag{B5}$$

In this case, for $\mu>\mu^h$ the ratio $(dh_T/d\Pi)/j_A<0$ and for $\mu<\mu^h$ the ratio $(dh_T/d\Pi)/j_A$ is positive.

*Electronic address: amoreira@cttmar.univali.br
†Electronic address: wagner@fisica.ufsc.br
‡Electronic address: vhenriques@if.usp.br

[1] J. M. Kincaid and E. G. D. Cohen, Phys. Rep., Phys. Lett. **22C**, 57 (1975).
[2] H. J. Herrmann, E. B. Rasmusseen, and D. P. Landau, J. Appl. Phys. **53**, 7994 (1982).
[3] D. P. Landau and R. H. Swendsen, Phys. Rev. Lett. **46**, 1437 (1987).
[4] H. J. Herrmann and D. P. Landau, Phys. Rev. B **48**, 239 (1993).
[5] W. Selke, Z. Phys. B: Condens. Matter **101**, 145 (1996).
[6] M. Pleimling and W. Selke, Phys. Rev. B **56**, 8855 (1997).
[7] M. Santos and W. Figueiredo, Phys. Rev. B **58**, 9321 (1998).
[8] M. Zukovic and T. Idogaki, Phys. Rev. B **61**, 50 (2000).
[9] V. A. Schmidt and S. A. Friedberg, Phys. Rev. B **1**, 2250 (1970).
[10] E. Stryjewski and N. Giordano, Adv. Phys. **26**, 487 (1977).
[11] K. Katsumata, H. Aruga Katori, S. M. Shapiro, and G. Shirane, Phys. Rev. B **55**, 11 466 (1997); Ch. Binek, T. Kato, W. Kleemann, O. Petraci, D. Bertrand, F. Bourdarot, P. Burlet, H. Aruga Katori, K. Katsumata, K. Prokes, and S. Welzel, Eur. Phys. J. B **15**, 35 (2000).
[12] W. P. Wolf, Braz. J. Phys. **30**, 794 (2000).
[13] C. Domb, J. Chem. Phys. **25**, 783 (1956).
[14] G. Baker and J. W. Essam, Phys. Rev. Lett. **24**, 447 (1970).
[15] J. Oitmaa and M. N. Barber, J. Phys. C **8**, 3653 (1975).
[16] D. J. Bergman and B. I. Halperin, Phys. Rev. B **13**, 2145 (1976).
[17] J. Bruno and J. Sak, Phys. Rev. B **22**, 3302 (1980).
[18] B. K. Chakrabarti, N. Bhattacharyya, and S. K. Sinha, J. Phys. C **15**, L777 (1982).
[19] V. B. Henriques and S. R. Salinas, J. Phys. C **20**, 2415 (1987).
[20] V. B. Henriques, Ph.D. thesis, Universidade de São Paulo, 1988.
[21] B. Grossmann and D. G. Rancourt, Phys. Rev. B **54**, 12 294 (1996); P. Massimino and H. T. Diep, J. Appl. Phys. **87**, 7043 (2000); E. H. Boubcher, P. Massimino, and H. T. Diep, J. Magn. Magn. Mater. **223**, 163 (2001).
[22] S. S. Uda and W. Figueiredo, Phys. Lett. A **117**, 372 (1986).
[23] C. Vettier, H. L. Alberts, and D. Bloch, Phys. Rev. Lett. **31**, 1414 (1973).
[24] S. Salem-Sughi, W. A. Ortiz, and A. D. Alvarenga, Phys. Rev. B **40**, 2589 (1989).
[25] S. Salem-Sughi and W. A. Ortiz, Phys. Rev. B **43**, 5784 ()1991.
[26] L. D. Landau, *Collected Papers* (Gordon and Breach, New York, 1967).
[27] A. F. S. Moreira, W. Figueiredo, and V. B. Henriques, Eur. Phys. J. B **27**, 153 (2002).